that the rate constant is also affected by the E_a of the reaction.[68] It is derived from the Collins–Kimball equation (Eq. 2) by using τ instead of D_r, with the assumption that D_r is inversely correlated with τ.

$$k_{obs} = k_{act}\left(\frac{\alpha T\left(\frac{1}{\tau}\right)^{\xi}}{k_{act} + \alpha T\left(\frac{1}{\tau}\right)^{\xi}}\right) \qquad (10)$$

Here, k_{act} is the rate constant without restriction of diffusion, as represented by Eq. (3), and α is a constant representing the correlation between τ and the diffusion-controlled rate. When k_{act} is much greater than diffusion-controlled rate ($k_{act} \gg \alpha T/\tau^{\xi}$), such that k_{obs} is not affected by E_a, Eq. (10) can be written as $k_{obs} = \alpha T/\tau^{\xi}$. Thus, αT in Eq. (10) corresponds to $A_k\tau_0^g$ in Eq. (9), and similarly, ξ corresponds to g. A smaller value of α means a smaller value of $A_k\tau_0^g$, which suggests that the number of diffusional jumps needed to complete the reaction is larger. Figure 17 shows the temperature dependence of rate constant (k_{obs}) simulated using representative values of E_a.[69] Here, k_{obs} is represented by t_{90} (the time required for 10% degradation). As E_a decreases, the significance of molecular mobility becomes greater, resulting in a more obvious change in the slope of temperature dependence around T_g. In addition, the significance of molecular mobility also depends on the values of α and ξ, such that a decrease in α and increase in ξ result in increased significance of molecular mobility.

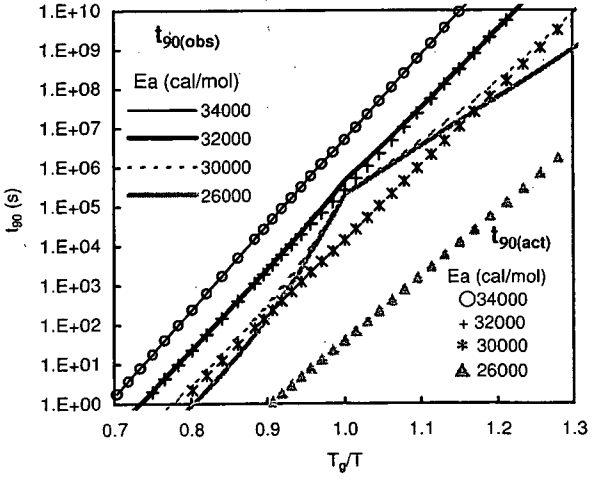

Figure 17. The effect of E_a on the temperature dependence of t_{90}. $t_{90(obs)}$ was calculated from k_{obs} using Eq. (10) with $\alpha = 5 \times 10^{-8}$ deg^{-1} and $\xi = 0.75$, and represented by lines. $t_{90(act)}$ was calculated from k_{act} using Eq. (3), and represented by symbols. (Reproduced from Reference [69] with permission of copyright owner.)

The rate of degradation of insulin lyophilized with PVP or dextran (main pathway: A21-deamidation and dimerization via a cyclic anhydride intermediate) was found to exhibit no significant change in the slope of temperature dependence around T_g.[68,70] Figure 18 shows the t_{90} of the PVP formulation, calculated from the apparent first-order rate constant obtained in the initial stage of degradation. Furthermore, the value of t_{90} at T_g varied greatly depending on humidity. These findings indicate that the degradation rate is not affected by global mobility, and that the rate is determined only by E_a. At low humidity, in contrast, the trehalose formulation exhibited an obvious change in the slope of temperature dependence around T_g (Fig. 18), which suggests that the effect of global mobility is significant. However, the β-relaxation of the insulin molecule, rather than global mobility, was found to determine the degradation rate at low humidity, as described below in the section regarding local mobility of amorphous pharmaceuticals. The obvious change in slope observed around T_g may be attributed to a possible coupling between global mobility and β-relaxation. The relative significance of E_a and β-relaxation in the insulin degradation rate was calculated according to the modified Collins–Kimball equation (Eq. 10) with the assumption that the temperature dependence of β-relaxation time can be approximated by that of structural relaxation time within the limited temperature range near T_g.[68,70] The value of k_{obs}/k_{act} was small at low humidity (Fig. 19) (unpublished data), indicating that the main determinant of the degradation rate is β-relaxation time, rather than the chemical activational barrier. The longer t_{90} of the trehalose formulation compared with the PVP formulation at a given temperature can be explained by the stronger ability of trehalose to hinder β-relaxation of the insulin molecule, as described below in the section regarding local mobility.

Temperature Dependence of Global Mobility

Because of the significant effect of global mobility on chemical reactivity, as described above, an understanding of the temperature dependence of global mobility is indispensable for predicting the stability of amorphous pharmaceuticals. The temperature dependence of structural relaxation time (τ) for various amorphous materials[71] has been described using the WLF equation (Eq. 1)

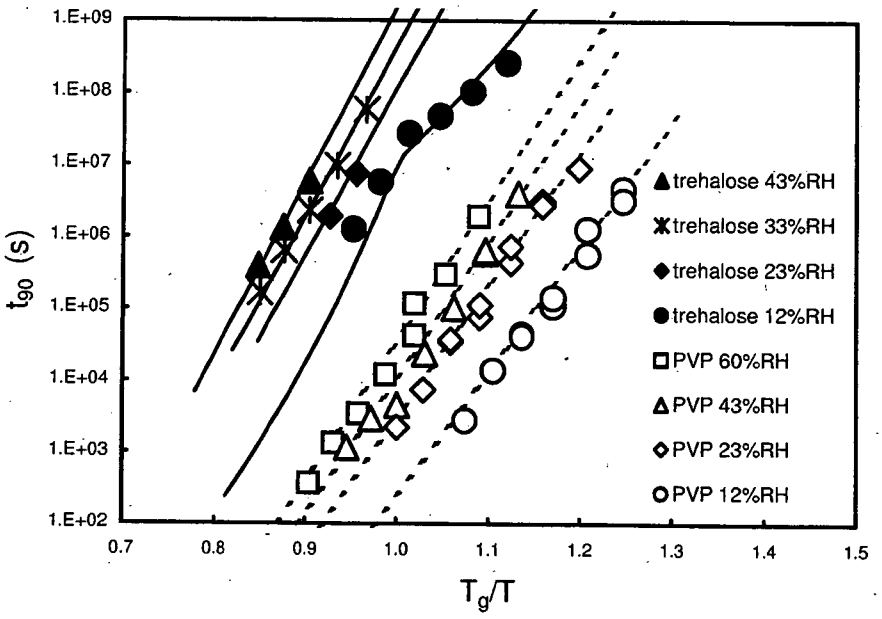

Figure 18. The rate-T_g/T plots for degradation of insulin lyophilized trehalose or PVP formulations. t_{90} was calculated from the apparent first-order rate constant obtained in the initial stage of degradation. (Produced using data reported in Reference [68,70].)

developed for mechanical and electrical relaxation.[72] The temperature dependence of τ can also be described using the Vogel–Tammann–Fulcher (VTF) equation (Eq. 11), which is roughly equivalent to the WLF equation.

$$\tau = \tau_0 \exp\left(\frac{DT_0}{T - T_0}\right) \qquad (11)$$

The VTF equation has been used to describe the temperature dependence of τ of amorphous

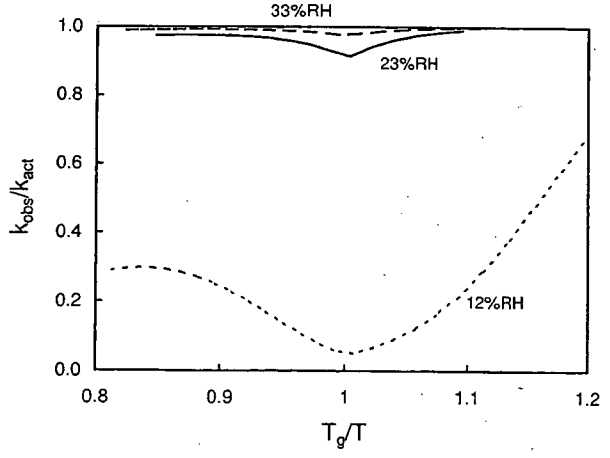

Figure 19. The significance of molecular mobility for the degradation rate of insulin lyophilized with trehalose as a function of T_g/T, as indicated by the ratio of k_{obs} to k_{act}. (Produced using data reported in Reference [68].)

indomethacin calculated from viscosity and frequency-dependent shear modulus at temperatures near and above T_g.[73]

Global mobility, as indicated by τ, in amorphous pharmaceuticals at temperatures below T_g can be determined from enthalpy relaxation time, which can be measured by conventional DSC, modulated temperature DSC[74,75] and isothermal microcalorimetry.[76,77] The enthalpy relaxation times measured for amorphous indomethacin, PVP and sucrose indicated that significant global mobility may be expected even at temperatures well below T_g.[78] The enthalpy relaxation times of amorphous benzodiazepines also indicated that global mobility is significant at temperatures below T_g.[79]

The temperature dependence of global mobility in amorphous pharmaceuticals may also be calculated according to the AGV equation (Eq. 5) by using experimentally determined values of D, T_0, and T_f.[80,81] The value of fragility, which is necessary to calculate the values of D and T_0, can be measured by various methods, such as those based on the width of glass transition, the heating-rate dependence of T_g, and configurational entropy.[82–84]

Shamblin et al.[63] calculated the structural relaxation times of indomethacin, sucrose, trehalose and sorbitol glasses using the AGV equation, and obtained values of T_k (T_0) ranging from 40 to 190 K below the T_g. The structural relaxation time

DOI 10.1002/jps

was estimated to be 3–5 years at T_k, which suggests that storage at temperatures below T_k is necessary to ensure shelf-life stability. For stability prediction of pharmaceutical products, the distribution of τ should be taken into account, because the values of τ obtained from enthalpy relaxation time and those calculated using the AGV equation v are mean relaxation times.[85,3b]

SIGNIFICANCE OF LOCAL MOBILITY FOR CHEMICAL REACTIVITY OF AMORPHOUS PHARMACEUTICALS

In addition to global mobility described above, the local mobility of drug and excipient molecules has attracted attention as an important factor in chemical reactivity. This section describes the effect of local mobility on the chemical reactivity of amorphous pharmaceuticals. Here, local mobility (β-relaxation) is referred to as mobility with a time scale shorter than that of global mobility, but longer than that of fast dynamics (γ-relaxation, δ-relaxation, —) such as the rotational motion of small functional groups in the molecule (e.g., methyl group).

Correlation between Local Mobility and Chemical Reactivity

The molecular motion required for a chemical reaction to proceed varies depending on the reaction mechanism. Correlations between chemical reactivity and local mobility have been demonstrated for several amorphous pharmaceuticals, although the available reported data are fewer than those related to correlations between chemical reactivity and global mobility.

Degradation of human insulin lyophilized from acidic solution involves deamidation at the Asn_{A21} position and covalent dimerization via formation of a cyclic anhydride intermediate at A21, which is the rate-determining step.[86] Based on the finding that formation of the intermediate occurred even in the glassy state, it was suggested that the conformational flexibility of the A21 segment, rather than global mobility, was important for reactivity. Furthermore, the primary degradation pathway of the cyclic anhydride intermediate in the glassy state was deamidation, which is thought to require only local mobility.[87] The importance of local mobility in insulin degradation is also suggested by the finding that amorphous insulin is far more stable than crystalline insulin, which has lower global mobility, indicating that stability is not determined by global mobility (Fig. 20).[88] As described in the previous section, the degradation rate of insulin lyophilized with dextran or PVP was affected only by the chemical activation energy and not by global mobility.[68,70] The degradation rate of insulin lyophilized with trehalose at low humidity, in contrast, was determined not only by the chemical activation energy but also by molecular mobility. The type of molecular mobility responsible for the degradation was found to be β-relaxation of the insulin molecule.[89] The rotating frame spin-lattice relaxation time ($T_{1\rho}$) of the insulin carbonyl carbon in the dextran formulation was equivalent to that determined for insulin alone, whereas spin-lattice relaxation was significantly retarded by the addition of trehalose, showing a longer $T_{1\rho}$ (Fig. 21). This indicates that β-relaxation is slower in the trehalose formulation than in the dextran formulation. It is suggested that trehalose has the ability to retard β-relaxation of the insulin molecule such that β-relaxation becomes the rate-determining process. The stabilizing effect of trehalose observed at low humidity was eliminated at higher humidity, in a similar manner to that in which the effect of trehalose in retarding β-relaxation of the insulin molecule at low humidity was eliminated at higher humidity. This finding supports the contention that β-relaxation, rather than global mobility, determines the degradation rate.

The significance of β-relaxation was also suggested in terms of the stability of lyophilized IgG1

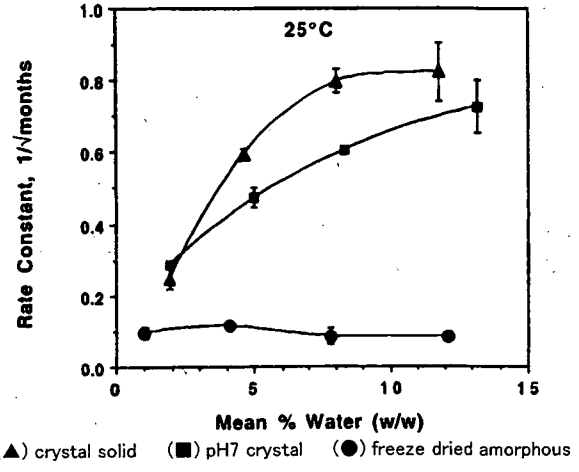

Figure 20. The effect of water content on the rate constant for A-21 deamidation of insulin in the solid state. The rate constants refer to the pseudo rate constant for "square root of time" kinetics. (Reproduced from Reference [88] with permission of copyright owner.)

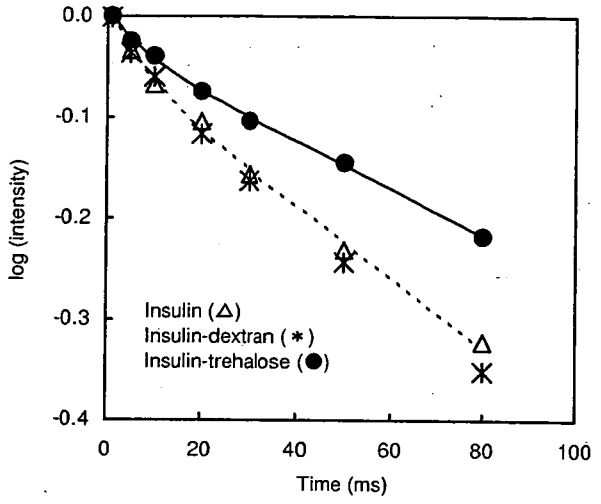

Figure 21. The time courses of rotating-frame spin-lattice relaxation for insulin carbonyl carbon in lyophilized insulin, insulin-dextran and insulin-trehalose systems. 25°C, 12% RH. (Reproduced from Reference [89] with permission of copyright owner.)

antibody.[90] The addition of a small amount of sorbitol was found to improve the storage stability of both IgG1-sucrose and IgG1-trehalose formulations, but addition of sorbitol decreased the structural relaxation times of both formulations. These findings indicate that there is no correlation between stability and global mobility. Furthermore, addition of sorbitol to the sucrose formulation resulted in greater retention of the native structure of the protein as determined by FTIR, but addition of sorbitol to the trehalose formulation had no effect on retention of the native structure, which indicates there is no correlation between stability and the retention of the native structure. Thus, molecular mobility other than global mobility (i.e., β-relaxation) is thought to be a critical factor in the stability of the protein.[90,91] Sorbitol has also been reported to reduce β-relaxation in a starch-water system.[92] Similar retarded β-relaxation has been observed in a glucose–water system.[93]

Coupling between Local Mobility and Global Mobility

Local mobility (β-relaxation), which may affect the chemical stability of amorphous pharmaceuticals depending on their degradation mechanisms, can be determined by dielectric relaxation[93,94] and NMR relaxation[95,96] measurements. Local mobility, involving motions on a smaller scale than that of global mobility, is thought to be coupled with global mobility,[4,97] although only limited data are available in this regard. The local mobility of lyophilized dextran, PVP and methylcellulose, determined based on the T_1 and $T_{1\rho}$ of the carbonyl carbon or methine carbon of the polymer, was found to increase abruptly, in association with an increase in global mobility, when the temperature rose above T_g, which suggests that local mobility is coupled with global mobility.[98–100] Coupling between local mobility and global mobility was also observed for γ-globulin lyophilized with dextran.[101] The temperature dependence of β-relaxation as determined by the T_1 of the protein carbonyl carbon exhibited an abrupt change around T_g, in a similar manner to that of β-relaxation determined by the T_1 of the dextran methine carbon. Coupling between local mobility and global mobility was also suggested by the finding that the degradation rate of insulin lyophilized with trehalose, which was found to be determined by the β-relaxation of the insulin molecule (as measured by the $T_{1\rho}$ of the insulin carbonyl carbon), exhibited a obvious change in temperature dependence around T_g.[68]

EXAMPLES FOR CHEMICAL STABILITY NOT APPARENTLY RELATED TO GLOBAL MOBILITY

Whereas many stability studies have demonstrated that there is a possible relationship between chemical stability and global mobility for various amorphous systems, as described above, the lack of apparent correlation between these factors have also been reported for many systems. For some cases, the lack of correlation can be explained in terms of local mobility responsible for the chemical reactivity, as described in the preceding section. However, other factors can also be responsible for the lack of apparent correlation between chemical stability and global mobility. The degradation rate of quinapril lyophilized with β-cyclodextrin was found to decrease with increasing β-cyclodextrin content up to a molar ratio of 1:1, regardless of decreasing T_g.[102] The effect of β-cyclodextrin in stabilizing the drug through complexation was more intense than the effect in decreasing the matrix T_g (Fig. 22).

The hydrolysis rate of 2-(4-nitrophenoxy)tetrahydropyran lyophilized with carbohydrates such as Ficoll decreased with decreases in carbohydrate

DOI 10.1002/jps

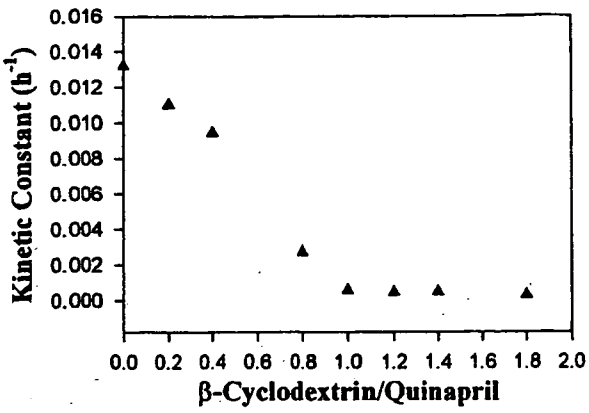

Figure 22. The effect of β-cyclodextrin on the rate constant for quinapril intramolecular cyclization at 80°C. (Reproduced from Reference [102] with permission of copyright owner.)

molecular weights, regardless of decreasing T_g.[103] The difference in the stabilizing effects of the various carbohydrates has been attributed to differences in the matrix density.

Variations in chemical stability that do not seem to be related to global mobility have also been observed for various solid proteins, including restriction enzyme EcoRI dried with sucrose, trehalose, maltodextrin or PVP,[104] lactase and invertase lyophilized with trehalose, maltose, lactose, sucrose, raffinose, maltodextrin, casein or PVP,[22,105–108] and glucose-6-phosphate dehydrogenase lyophilized with dextran, sucrose or raffinose.[109–110] It is not easy to explain the lack of correlation between chemical stability and global mobility for proteins because of many complicated factors possibly affecting the chemical stability. Protein structural changes arising during the lyophilization process may affect stability during subsequent storage.[111–115]

The lack of correlation between chemical stability and global mobility observed for several amorphous systems has been explained by the contribution of excipient as reactant, complicated effects of water, and the heterogeneity of amorphous matrix, as described below.

The Role of Excipients as Reactants

The storage stability of amorphous pharmaceuticals in which an excipient is involved in the chemical degradation as a reactant may not be related to global mobility. When glucose, a reducing sugar, was used as an excipient in lyophilized recombinant human relaxin formulation, covalent adducts of glucose with amino groups on the side chains of the protein were formed via the Maillard reaction.[116] In addition, glucose was found to react with the Ser hydroxy group and to cause Ser cleavage from the C-terminal of the B-chain of relaxin. Another example of the effect of an excipient as a reactant has been reported for sucrose lyophilized with ribonuclease A.[117] Sucrose lyophilized from acid solutions is thought to hydrolyze to glucose and fructose, which undergo further degradation, resulting in enhancement of protein degradation.

Complex Effects of Water

The effect of water on the storage chemical stability of amorphous pharmaceuticals is not simple; water can act not only as a plasticizer, but also as a reactant or medium.[51,118,119] These complicated effects of water may also be responsible for an apparent lack of relationship between chemical stability and global mobility. It has been found that the degradation rate of aspartame lyophilized with PVP is not related to the value of temperature relative to T_g ($T-T_g$), and the degradation rate changed with differing water activity, even when T_g is the same.[120,121]

For diffusion-controlled degradation involving water as a reactant, the rate should depend on the diffusion rate of water. However, no apparent relationship between chemical stability and matrix T_g is expected, unless the diffusion rate of water is related to T_g. Various physical states of water with differing molecular mobilities have been observed in polymer-water systems by DRS and NMR.[122–124] Based on molecular dynamics simulations, water distribution in PVP glasses was suggested to be highly heterogeneous at 10% w/w water content.[125] Water molecules are known to have high diffusivity even in amorphous solids. Water in solid amorphous Ficoll[126] and carbohydrates[127] was found to have diffusivity values high enough to be determined from the rate of desorption even at temperatures below T_g; the diffusion constants of water exhibited linear Arrhenius behavior around T_g. The diffusion coefficient of water in solid PVP, determined by the absorption-desorption technique for smaller water contents and by the pulsed field gradient spin echo technique for larger contents, exhibited no changes in water-content dependence around W_g (the amount of water necessary to depress T_g to the

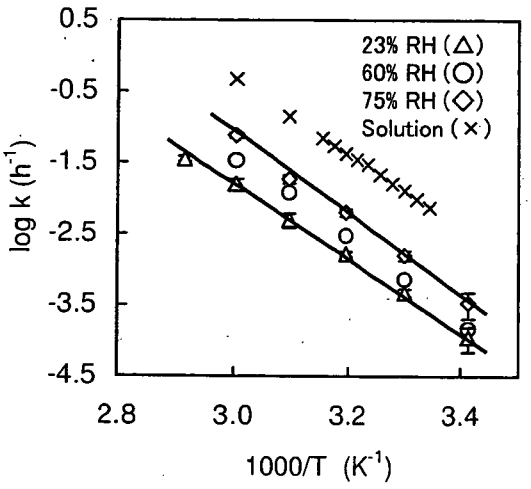

Figure 23. The Arrhenius plots for hydrolysis of cephalothin lyophilized with dextran. (Reproduced from Reference [10] with permission of copyright owner.)

isotherm temperature), indicating that water molecules have high translational mobility even in the glassy state.[128] The high diffusivity of water molecules even at temperatures below T_g can explain the lack of an apparent relationship between chemical stability and global mobility when water acts as a reactant in the degradation of amorphous pharmaceuticals. The hydrolysis rate of cephalothin in dextran matrices exhibited temperature dependence which was unaffected by T_{mc} (55°C, 35° and 22° at 23, 60, and 75% RH, respectively), as shown in Figure 23.[10]

Heterogeneity of Amorphous Matrix

The heterogeneity of amorphous matrices is another explanation for cases in which no relationship is observed between chemical stability and global mobility. When the amorphous matrix contains crystalline phases that undergo degradation, the apparent degradation rate is not necessarily related to T_g. The rate of solid-state methyl transfer in tetraglycine methyl ester was faster in the amorphous matrices prepared by freeze-drying than in those prepared by milling, because fast degradation occurred in the crystalline phases coexisting in the amorphous matrices prepared by freeze-drying.[129,130]

Heterogeneity created during chemical reactions may also be responsible for a lack of apparent relationship between chemical stability and global mobility. The chemical degradation rate of amorphous sodium indomethacin was found to be unrelated to T_g, with a greater rate observed at low humidities than at high humidities.[131] This can be attributed to formation of the more chemically stable crystalline phase at higher humidities. The effects of heterogeneity created during chemical reactions have also been reported for degradation of tetraglycine methyl ester[132] and aspartame.[133] Amorphous matrices with an appropriate distribution of reactants may also exhibit high reactivity even at temperatures below T_g, displaying temperature dependence that is not related to T_g, as exemplified by the oxidation of solid-state human insulin-like growth factor I.[134]

SUMMARY

Literature describing the storage chemical stability of amorphous pharmaceuticals in relation to molecular mobility was reviewed to clarify the degree of our understanding about correlations between chemical stability and molecular mobility, and to highlight the need for future studies on this subject. The chemical reactivity of amorphous pharmaceuticals is determined by the relative effects of the chemical activational barrier and molecular mobility. The significance of molecular mobility is greatly affected by the value of E_a of the degradation, in that an increase in E_a reduces the significance of molecular mobility. When the effect of molecular mobility on chemical reactivity is negligible compared with that of thermodynamic factors, the chemical stability of the formulation can be predicted by extrapolating data obtained at elevated temperatures through the T_g.

The significance of molecular mobility for chemical reactivity is also determined by the mechanism of degradation, in other words, the length scale of molecular mobility responsible for the chemical reactivity. Global mobility is predominant in determining the rate of degradation for bimolecular reactions, in which diffusion of the reactants is the rate-determining step, as exemplified by acetyl transfer between aspirin and sulfadiazine. In contrast, local mobility is an important determinant of the degradation rate for mechanisms requiring smaller-scale motion, as exemplified by degradation of insulin via formation of a cyclic anhydride intermediate. Even if local mobility rather than global mobility is responsible for the degradation, reactivity may exhibit changes in the slope of temperature dependence around T_g. This apparent relationship between reactivity and matrix T_g may be

DOI 10.1002/jps

DOI 10.1002/jps

Table 1. Representative Amorphous Systems Classified According to the Type of Molecular Mobility Relevant to the Degradation

Most Relevant Molecular Mobility or Other Factors	System	Degradation	References
Global mobility (suggested from correlation between degradation rate and $(T-T_g)$)	Lyophilized monoclonal antibody—vinca conjugate	Dimer formation, vinca generation, vinca decomposition	54
	Lyophilized glucose-6-phosphate dehydrogenase	Inactivation	55
	Lyophilized bovine γ-globulin—dextran system	Aggregation	56
	Lyophilized Asn-hexapeptide–PVP/glycerin system	Deamidation in rubbery state	57,58
Global mobility (suggested from correlation between degradation rate and structural relaxation time)	Lyophilized cephalospolines	Hydrolysis in lyophilized formulation	3b
	Amorphous quinapril hydrochloride	Intramolecuar cyclization	66
	Lyophilized human growth hormone	Aggregation	3b
	Lyophilized IgG1—sucrose system	Aggregation	3b
Global mobility (suggested from non-linear behavior around T_g)	Lyophilized cefalothin sodium	Hydrolysis	8
	Lyophilized aspirin—hydroxypropyl-β-CyD system	Hydrolysis	9
	Lyophilized aspirin—sulfadiazine—dextran/methylcellulose system	Acetyl transfer reaction	10
	Lyophilized monoclonal antibody	Aggregation	13
	Lyophilized bovine γ-globulin—dextran/methyl cellulose system	Aggregation	16
	Lyophilized β-galactosidase—PVA/methyl cellulose system	Aggregation	17
Global mobility (suggested from decreased rate associated with increased T_g)	Lyophilized glycin-glucose—PVP system	Maillard reaction	19
	Lyophilized invertase—PVP system	Inactivation	22
	Lyophilized recombinant interleukin-2—sugar system	Aggregation	23
	Lyophilized actin—disaccharide—dextran system	Aggregation	25
	Lyophilized human interleukin-11—disaccharide—hydroxyethyl starch system	Aggregation	26
	Lyophilized bovine γ-globulin—dextran system	Aggregation	24
Local mobility (suggested from NMR relaxation time)	Lyophilized insulin—trehalose system	Deamidation and dimerization via cyclic anhydride intermediate	89
Chemical activation energy	Lyophilized insulin—PVP /dextran system	Deamidation and dimerization via cyclic anhydride intermediate	68,70
	Lyophilized cephalothin—dextran system	Hydrolysis	10
	Lyophilized lysine-glucose system	Maillard reaction	62
Reaction involving excipient	Lyophilized quinapril—hydrochloride-β-CyD system	Intramolecular cyclization	102
	Lyophilized recombinant human relaxin—glucose system	Maillard reaction, Reaction between glucose and Ser-hydroxy group	116
	Lyophilized ribonuclease A—sucrose system	Reaction with glucose, degradation product of sucrose	117

explained in terms of coupling between local mobility and global mobility, although further studies about the temperature dependence of local mobility in comparison with that of global mobility are needed to confirm this coupling. Formulations exhibiting degradation with a significant contribution either from global or local mobility can be stabilized by using antiplasticizers to decrease global or local mobility.

Close relationships between chemical stability (orders of months and years) and global mobility (orders of 100 s at T_g) or local mobility (order of ms to μs), demonstrated for various amorphous systems, give rise of speculation that a number of diffusional jumps are needed to complete a degradation in the amorphous state, and that the rate of each jump is determined by global mobility or local mobility.

Storage at temperatures below T_k is considered appropriate in ensuring the shelf-life stability of amorphous pharmaceuticals in which degradation rate is affected by global mobility. However, this is not the case for amorphous pharmaceuticals in which the degradation rate is affected by local mobility, because local mobility may be sufficient for degradation to occur even at temperatures below T_k.

Another subject that needs to be studied may be to elucidate the effect of the heterogeneous properties of amorphous pharmaceuticals (e.g., microscopic phase separation) on their chemical reactivity.

Finally, the representative amorphous systems considered in this article are summarized in Table 1, classified according to the type of molecular mobility relevant to the degradation.

REFERENCES

1. Craig DQM, Royall PG, Kett VL, Hopton ML. 1999. The relevance of the amorphous state to pharmaceutical dosage forms: Glassy drugs and freeze dried systems. Int J Pharm 179:179–207.
2. Wang W. 2000. Lyophilization and development of solid protein pharmaceuticals. Int J Pharm 203: 1–60.
3. (a) Parker R, Gunning YM, Lalloué B, Noel TR, Ring SG. 2002. Glassy state dynamics, its significance for biostabilization and role of carbohydrates. In: Levine H, editor. Amorphous food and pharmaceutical systems. Cambridge: The Royal Society of Chemistry. pp 73–87.
   (b) Pikal MJ. 2002. Chemistry in solid amorphous matrices: Implication for biostabilization. In: Levine H, editor. Amorphous food and pharmaceutical systems. Cambridge: The Royal Society of Chemistry. pp 257–272.
4. Pikal MJ. 2004. Mechanisms of protein stabilization during freeze-drying and storage: The relative importance of thermodynamic stabilization and glassy state relaxation dynamics. In: Rey L, May JC, editors. Freeze-drying/lyophilization of pharmaceutical and biological products. 2nd edition. New York: Marcel Dekker Inc. pp 63–107.
5. (a) Shamblin SL. 2004. The role of water in physical transformations in freeze-dried products. In: Costantino HR, Pikal MJ, editors. Lyophilization of biopharmaceuticals. Arlington: AAPS Press. pp 229–270.
   (b) Lechuga-Ballesteros D, Miller DP, Duddu SP. 2004. Thermal analysis of lyophilized pharmaceutical peptide and protein formulations. In: Costantino HR, Pikal MJ, editors. Lyophilization of biopharmaceuticals. Arlington: AAPS Press. pp 271–335.
   (c) Stotz CE, Winslow SL, Houchin ML, D'Souza AJM, Ji J, Topp EM. 2004. Degradation pathways for lyophilized peptides and proteins. In: Costantino HR, Pikal MJ, editors. Lyophilization of biopharmaceuticals. Arlington: AAPS Press. pp 443–479.
6. Carpenter JF, Chang BS, Randolph TW. 2004. Physical damage to proteins during freezing, drying, and rehydration. In: Costantino HR, Pikal MJ, editors. Lyophilization of biopharmaceuticals. Arlington: AAPS Press. pp 423–442.
7. Oberholtzer ER, Brenner GS. 1979. Cefoxitin sodium: Solution and solid-state chemical stability studies. J Pharm Sci 68:863–866.
8. Pikal MJ, Lukes AL, Lang JE. 1977. Thermal decomposition of amorphous β-lactam antibacterials. J Pharm Sci 66:1312–1316.
9. Duddu SP, Weller K. 1996. Importance of glass transition temperature in accelerated stability testing of amorphous solids: Case study using a lyophilized aspirin formulation. J Pharm Sci 85:345–347.
10. Yoshioka S, Aso Y, Kojima S. 2000. Temperature dependence of bimolecular reactions associated with molecular mobility in lyophilized formulations. Pharm Res 17:925–929.
11. Yoshioka S, Aso Y, Kojima S. 1999. The effect of excipients on the molecular mobility of lyophilized formulations, as measured by glass transition temperature and NMR relaxation-based critical mobility temperature. Pharm Res 16:135–140.
12. Pikal MJ, Dellerman K, Roy ML. 1991. Formulation and stability of freeze-dried proteins: Effects of moisture and oxygen on the stability of freeze-dried formulations of human growth hormone. Develop Biol Standard 74:21–38.

DOI 10.1002/jps

13. Duddu SP, Dal Monte PR. 1997. Effect of glass transition temperature on the stability of lyophilized formulations containing a chimeric therapeutic monoclonal antibody. Pharm Res 14:591–595.
14. Yoshioka S, Aso Y, Kojima S. 1996. Determination of molecular mobility of lyophilized bovine serum albumin and γ-globulin by solid state ^{1}H-NMR and relation to aggregation-susceptibility. Pharm Res 13:926–930.
15. Yoshioka S, Aso Y, Kojima S. 1997. Softening temperature of lyophilized bovine serum albumin and γ-globulin as measured by spin-spin relaxation time of protein protons. J Pharm Sci 86:470–474.
16. Yoshioka S, Aso Y, Kojima S. 2001. Usefulness of Kohlrausch-Williams-Watts stretched exponential function to describe protein aggregation in lyophilized formulations and temperature dependence of near the glass transition temperature. Pharm Res 18:256–260.
17. Yoshioka S, Tajima S, Aso Y, Kojima S. 2003. Inactivation and aggregation of β-galactosidase in lyophilized formulation described by Kohlrausch-Williams-Watts stretched exponential function. Pharm Res 20:1655–1660.
18. Pikal MJ, Dellerman KM, Roy ML, Riggin RM. 1991. The effects of formulation variables on the stability of freeze-dried human growth hormone. Pharm Res 8:427–436.
19. Bell LN, Touma DE, White KL, Chen YH. 1998. Glycine loss and maillard browning as related to glass transition in a model food system. J Food Sci 63:625–628.
20. Guo Y, Byrn SR, Zografi G. 2000. Effects of lyophilization on the physical characteristics and chemical stability of amorphous quinapril hydrochloride. Pharm Res 17:930–935.
21. Li J, Guo Y, Zografi G. 2002. Effects of a citrate buffer system on the solid-state chemical stability of lyophilized quinapril preparation. Pharm Res 19:20–26.
22. Schebor C, Buera MP, Chirife J. 1996. Glassy state in relation to thermal inactivation of the enzyme invertase in amorphous dried matrices of trehalose, maltodextrin and PVP. J Food Eng 30:269–282.
23. Prestrelski SJ, Pikal KA, Arakawa T. 1995. Optimization of lyophilization conditions for recombinant human interleukin-2 by dried-state conformational analysis using fourier-transform infrared spectroscopy. Pharm Res 12:1250–1259.
24. Yoshioka S, Aso Y, Kojima S. 1997. Dependence of molecular mobility and protein stability of freeze-dried γ-globulin formulations on the molecular weight of dextran. Pharm Res 14:736–741.
25. Allison SD, Manning M, Randolph TW, Middleton K, Davis A, Carpenter JF. 2000. Optimization of storage stability of lyophilized actin using combinations of disaccharides and dextran. J Pharm Sci 89:199–214.
26. Garzon-Rodriguez W, Koval RL, Chongprasert S, Krishman S, Randolph TW, Warne NW, Carpenter JF. 2004. Optimizing storage stability of lyophilized recombinant human interleukin-11 with disaccharide/hydroxyethyl starch mixtures. J Pharm Sci 93:684–696.
27. Oksanen CA, Zografi G. 1990. The relationship between the glass transition temperature and water vapor absorption by poly(vinylpyrrolidone). Pharm Res 7:654–657.
28. Ahlneck C, Zografi G. 1990. The molecular basis of moisture effects on te physical and chemical stability of drugs in the solid state. Int J Pharm 62:87–95.
29. Hancock BC, Zografi G. 1994. The relationship between the glass transition temperature and water content of amorphous pharmaceutical solids. Pharm Res 11:471–477.
30. Shamblin SL, Hancock BC, Zografi G. 1998. Water vapor sorption by peptide, protein and their formulations. Eur J Pharm Biopharm 45:239–247.
31. Slade L, Levine H. 1991. Beyond water activity: Recent advances based on an alternative approach to the assessment of food stability and safety. Crit Rev Food Sci Nutri 30:115–360.
32. Slade L, Levine H. 1995. Glass transitions and water-food structure interactions. In: Kinsella JE, Taylar SL, editors. Advances in Food and Nutrition Research. Vol. 38. New York: Academic Press Inc. pp 103–269.
33. Kararli TT, Catalano T, Needham TE, Finnegan PM. 1991. Mechanism of misoprostol stabilization in hydroxypropyl methylcellulose. In: Levine H, Slade L, editors. Water relationship in food. New York: Plenum Press. pp 275–289.
34. Kararli TT, Catalano T. 1990. Stabilization of misoprostol with hydroxypropyl methylcellulose (HPMC) against degradation by water. Pharm Res 7:1186–1189.
35. Townsend MW, DeLuca PP. 1990. Stability of ribonuclease A in solution and freeze-dried state. J Pharm Sci 79:1083–1086.
36. Hsu CC, Ward CA, Pearlman R, Nguyen HM, Yeung DA, Curley JG. 1991. Determining the optimum residual moisture in lyophilized protein pharmaceuticals. Develop Biol Standard 74:255–271.
37. Hageman MJ, Possert PL, Bauer JM. 1992. Prediction and characterization of the water sorption isotherm for bovine somatotropin. J Agric Food Chem 40:342–347.
38. Chan H, Clark AR, Feeley J, Kuo M, Lehrman SR, Pikal-Cleland K, Miller DP, Vehring R, Lechuga-Ballesteros D. 2004. Physical stability of salmon calcitonin spray-dried powder for inhalation. J Pharm Sci 93:792–804.

39. Constantino HR, Langer R, Klibanov AM. 1994. Moisture-induced aggregation of lyophilized insulin. Pharm Res 11:21–29.
40. Constantino HR, Langer R, Klibanov AM. 1994. Solid-phase aggregation of proteins under pharmaceutically relevant conditions. J Pharm Sci 83: 1662–1669.
41. Liu WR, Langer R, Klibanov AM. 1991. Moisture-induced aggregation of lyophilized proteins in the solid state. Biotechnol Bioeng 37:177–184.
42. Jordan GM, Yoshioka S, Terao T. 1994. The aggregation of bovine serum albumin in solution and in the solid state. J Pharm Pharmacol 46:182–185.
43. Constantino HR, Langer R, Klibanov AM. 1995. Aggregation of a lyophilized pharmaceutical protein, recombinant human albumin: Effect of moisture and stabilization by excipients. Biotechnology 13:493–496.
44. Schwendeman SP, Constantino HR, Gupta RK, Siber G, Klibanov AM, Langer R. 1995. Stabilization of tetanus and diphtheria toxoids against moisture-induced aggregation. Proc Natl Acad Sci USA 92:11234–11238.
45. Constantino HR, Schwendeman SP, Griebenow K, Kilibanov AM, Langer R. 1996. Secondary structure and aggregation of lyophilized tetanus toxoid. J Pharm Sci 85:1290–1293.
46. Katakam M, Banga AK. 1995. Aggregation of insulin and its prevention by carbohydrate excipients. PDA J Pharm Sci Technol 49:160–165.
47. Katakam M, Banga AK. 1995. Aggregation of proteins and its prevention by carbohydrate excipients: Albumins and γ-globulin. J Pharm Pharmacol 47:103–107.
48. Chang BS, Reeder G, Carpenter JF. 1996. Development of a stable freeze-dried formulation of recombinant human interleukin-1 receptor antagonist. Pharm Res 13:243–249.
49. Byrn SR, Xu W, Newman AW. 2001. Chemical reactivity in solid-state pharmaceuticals: Formulation implications. Adv Drug Deliv Rev 48:115–136.
50. Herman BD, Sinclair BD, Milton N, Nail SL. 1994. The effect of bulking agent on the solid-state stability of freeze-dried methylprednisolone sodium succinate. Pharm Res 11:1467–1473.
51. Shalaev EY, Zografi G. 1996. How does residual water affect the solid-state degradation of drugs in the amorphous state? J Pharm Sci 85:1137–1141.
52. Separovic F, Lam YH, Ke X, Chan H-K. 1998. A solid-state NMR study of protein hydration and stability. Pharma Res 15:1816–1821.
53. Lam YH, Bustami R, Phan T, Chan H-K, Separovic F. 2002. A solid-state NMR study of protein mobility in lyophilized protein-sugar powders. J Pharm Sci 91:943–951.
54. Roy ML, Pikal MJ, Rickard EC, Malony AM. 1991. The effect of formulation and moisture on the stability of a freeze-dried monoclonal antibody-vinca conjugate: A test of the WLF glass transition theory. Devlop Biol Standard 74:323–340.
55. Sun WQ, Davidson P, Chan HSO. 1998. Protein stability in the amorphous carbohydrate matrix: Relevance to anhydrobiosis. Biochim Biophys Acta 1425:245–254.
56. Yoshioka S, Aso Y, Nakai Y, Kojima S. 1998. Effect of high molecular mobility of poly(vinyl alcohol) on protein stability of lyophilized γ-globulin formulations. J Pharm Sci 87:147–151.
57. Lai MC, Hageman MJ, Schowen RL, Borchardt RT, Topp EM. 1999. Chemical stability of peptide in polymers. 1. Effect of water on peptide deamidation in poly(vinyl alcohol) and poly(vinylpyrrolidone) matrices. J Pharm Sci 88:1073–1080.
58. Lai MC, Hageman MJ, Schowen RL, Borchardt RT, Laird BB, Topp EM. 1999. Chemical stability of peptide in polymers. 2. Discriminating between solvent and plasticizing effects of water on peptide deamidation in poly(vinylpyrrolidone). J Pharm Sci 88:1081–1089.
59. Yoshioka S, Aso Y, Kojima S. 2004. Temperature- and glass transition temperature-dependence of bimolecular reaction rates in lyophilized formulations described by the Adam-Gibbs-Vogel equation. J Pharm Sci 93:1062–1069.
60. Collins FC, Kimball GE. 1949. Diffusion-controlled reaction rates. J Colloid Sci 4:425–437.
61. Karel M, Saguy I, 1991. Effect of water on diffusion in food systems. Adv Exp Med Biol 302:157–173.
62. Craig ID, Parker R, Rigby NM, Cairns P, Ring SG. 2001. Maillard reaction kinetics in model preservation systems in the vicinity of the glass transition: Experiment and theory. J Agric Food Chem 49:4706–4712.
63. Shamblin SL, Tang X, Chang L, Hancock BC, Pikal MJ. 1999. Characterization for the time scales of molecular motion in pharmaceutically important glasses. J Phys Chem B 103:4113–4121.
64. Inoue T, Cicerone MT, Ediger MD. 1995. Molecular motions and viscoelasticity of amorphous polymers near T_g. Macromolecules 28:3425–3433.
65. Duddu SP, Zhang G, Dal Monte PR. 1997. The relationship between protein aggregation and molecular mobility below the glass transition temperature of lyophilized formulations containing a monoclonal antibody. Pharm Res 14:596–600.
66. Guo Y, Byrn SR, Zografi G. 2000. Physical characteristics and chemical degradation of amorphous quinapril hydrochloride. J Pharm Sci 89: 128–143.
67. Fujara F, Geil B, Sillescu H, Fleischer G. 1992. Translational and rotational diffusion in supercooled orthoterphenyl close to the glass

DOI 10.1002/jps

transition. Z Phys B Condensed Matter 88:195–204.
68. Yoshioka S, Aso Y. 2005. A quantitative assessment of the significance of molecular mobility as a determinant for the stability of lyophilized insulin formulations. Pharm Res 22:1358–1364.
69. Yoshioka S, Miyazaki T, Aso Y. 2006. Degradation rate of lyophilized insulin, exhibiting an apparent arrhenius behavior around glass transition temperature regardless of significant contribution of molecular mobility. J Pharm Sci 95:2684–2691.
70. Yoshioka S, Aso Y, Miyazaki T. 2006. Negligible contribution of molecular mobility to the degradation rate of insulin lyophilized with poly(vinylpyrrolidone). J Pharm Sci 95:939–943.
71. Peleg M. 1992. On the use of the WLF model in polymer and foods. Crit Rev Food Sci Nutr 32:59–66.
72. Williams ML, Landel RF, Ferry JD. 1955. The temperature dependence of relaxation mechanisms in amorphous polymers and other glass-forming liquids. J Am Chem Soc 77:3701–3707.
73. Andronis V, Zografi G. 1997. Molecular mobility of supercooled amorphous indomethacin, determination by dynamic mechanical analysis. Pharm Res 14:410–414.
74. Craig DQM, Barsnes M, Royall PG, Kett VL. 2000. An evaluation of the use of modulated temperature DSC as a means of assessing the relaxation behaviour of amorphous lactose. Pharm Res 17:696–700.
75. Van den Mooter G, Craig DQM, Royall PG. 2001. Characterization of amorphous ketoconazole using modulated temperature differential scanning calorimetry. J Pharm Sci 90:996–1003.
76. Liu J, Rigsbee DR, Stotz C, Pikal MJ. 2002. Dynamics of pharmaceutical amorphous solids: The study of enthalpy relaxation by isothermal microcalorimetry. J Pharm Sci 91:1853–1862.
77. Kawakami K, Ida Y. 2003. Direct observation of the enthalpy relaxation and the recovery processes of maltose-based amorphous formulation by isothermal microcalorimetry. Pharm Res 20:1430–1436.
78. Hancock BC, Shamblin SL, Zografi G. 1995. Molecular mobility of amorphous pharmaceutical solids below their glass transition temperatures. Pharm Res 12:799–806.
79. Van den Mooter G, Augustijns P, Kinget R. 1999. Stability prediction of amorphous benzodiazepies by calculation of the mean relaxation time constant using Williams-Watts-decay function. Eur J Pharm Biopharm 48:43–48.
80. Hodge IM. 1995. Physical aging in polymer glasses. Science 267:1945–1947.
81. Tong P, Zografi G. 1999. Solid-state characteristics of amorphous sodium indomethacin relative to its free acid. Pharm Res 16:1186–1192.
82. Crowley KJ, Zografi G. 2001. The use of thermal methods for predicting glass-former fragility. Thermochimica Acta 380:79–93.
83. Pikal MJ, Chang L, Tang X. 2004. Evaluation of glassy-state dynamics from the width of glass transition: Results from theoretical simulation of differential scanning calorimetry and comparison with experiments. J Pharm Sci 93:981–994.
84. Hancock BC, Christensen K, Shamblin SL. 1998. Estimating the critical molecular mobility temperature (T_k) of amorphous pharmaceuticals. Pharm Res 15:1649–1651.
85. Shamblin SL, Hancock BC, Dupuis Y, Pikal MJ. 2000. Interpretation of relaxation time constants for amorphous pharmaceutical systems. J Pharm Sci 89:417–427.
86. Strickley RG, Anderson BD. 1996. Solid-state stability of human insulin I. Mechanism and the effect of water on kinetics of degradation in lyophiles from pH 2–5 solutions. Pharm Res 13:1142–1153.
87. Strickley RG, Anderson BD. 1997. Solid-state stability of human insulin II. Effect of water on reactive intermediate partitioning in lyophiles from pH 2-5solutions: Stabilization against covalent dimer formation. J Pharm Sci 86:645–653.
88. Pikal MJ, Rigsbee DR. 1997. The stability of insulin in crystalline and amorphous solid: Observation of greater stability for the amorphous form. Pharm Res 14:1379–1387.
89. Yoshioka S Miyazaki T, Aso Y. 2006. β-Relaxation of insulin molecule in lyophilized formulations containing trehalose or dextran as a determinant of chemical reactivity. Pharm Res 23:961–966.
90. Chang L, Shepherd D, Sun J, Ouellette D, Grant KL, Tang X, Pikal MJ. 2005. Mechanism of protein stabilization by sugar during freeze-drying and storage: Native structure preservation, specific interaction, and/or immobilization in a glassy matrix? J Pharm Sci 94:1427–1444.
91. Chang L, Shepherd D, Sun J, Tang X, Pikal MJ. 2005. Effect of sorbitol and residual moisture on the stability of lyophilized antibodies: Implications for the mechanism of protein stabilization in the solid state. J Pharm Sci 94:1445–1455.
92. Gandin S, Lourdin D, Forssell PM, Colonna P. 2000. Antiplasticisation and oxygen permeability of starch-sorbitol films. Carbohydr Polym 43: 33–37.
93. Noel TR, Parker R, Ring SG. 1996. A comparative study of the dielectric relaxation behaviour of glucose, maltose, and their mixtures with water in the liquid and glassy states. Carbohydrate Res 282:193–206.
94. Noel TR, Parker R, Ring SG. 2000. Effect of molecular structure and water content on the dielectric relaxation behaviour of amorphous low molecular weight carbohydrates above and below

their glass transition. Carbohydr Res 329:839–845.
95. Masuda K, Tabata S, Sakata Y, Hayase T, Yonemochi E, Terada K. 2005. Comparison of molecular mobility in the glassy state between amorphous indomethacin and salicin based on spin-lattice relaxation times. Pharm Res 22:797–805.
96. Aso Y, Yoshioka S, Zhang J, Zografi G. 2002. Effect of water on molecular mobility of sucrose and poly(vinylpyrrolidone) in a colyophilized formulation as measured by ^{13}C-NMR relaxation time. Chem Pharm Bull 50:822–826.
97. Fujiwara T, Nagayama K. 1985. The wobbling-in-a-cone analysis of internal motion in macromolecules. J Chem Phys 83:3110–3117.
98. Yoshioka S, Aso Y, Kojima S. 2002. Different molecular motions in lyophilized protein formulations as determined by laboratory and rotating frame spin-lattice relaxation times. J Pharm Sci 91:2203–2210.
99. Yoshioka S, Aso Y, Kojima S. 2003. Molecular mobility of lyophilized Poly(vinylpyrrolidone) and methylcellulose as determined by the laboratory and rotating frame spin-lattice relaxation times of ^{1}H and ^{13}C. Chem Pharm Bull 51:1289–1292.
100. Yoshioka S, Aso Y. 2005. Glass transition-related changes in molecular mobility below glass transition temperature of freeze-dried formulations, as measured by dielectric spectroscopy and solid state nuclear magnetic resonance. J Pharm Sci 94:275–287.
101. Yoshioka S, Aso Y, Kojima S, Sakurai S, Fujiwara T, Akutsu H. 1999. Molecular mobility of protein in lyophilized formulations linked to the molecular mobility of polymer excipients, as determined by high resolution ^{13}C solid-state NMR. Pharm Res 16:1621–1625.
102. Li J, Guo Y, Zografi G. 2002. The solid-state stability of amorphous quinapril in the presence of β-cyclodextrins. J Pharm Sci 91:229–243.
103. Streefland L, Auffret AD, Franks F. 1998. Bond cleavage reactions in solid aqueous carbohydrate solutions. Pharm Res 15:843–849.
104. Rossi R, Buera MP, Moreno S, Chirife J. 1997. Stabilization of restriction enzyme *Eco*RI dried with trehalose and other selected glass-forming solutes. Biotechnol Prog 13:609–616.
105. Cardona S, Schebor C, Buera MP, Karel M, Chirife J. 1997. Thermal stability of invertase in reduced-moisture amorphous matrices in relation to glassy state and trehalose crystallization. J Food Sci 62: 105–112.
106. Mazzobre MF, Buera MP, Chirife J. 1997. Glass transition and thermal stability of lactase in low-moisture amorphous polymeric matrices. Biotecnol Prog 13:195–199.
107. Schebor C, Burin L, Buera MP, Aguilera JM, Chirife J. 1997. Glassy state and thermal inactivation of invertase and lactase in dried amorphous matrices. Biotecnol Prog 13:857–863.
108. Chen Y-H, Aull JL, Bell LN. 1999. Invertase storage stability and sucrose hydrolysis in solids as affected by water activity and glass transition. J Agric Food Chem 47:504–509.
109. Sun WQ, Davidson P. 2001. Effect of dextan molecular weight on protein stabilization during freeze-drying and storage. Cryo Lett 22:285–292.
110. Davidson P, Sun WQ. 2001. Effect of sucrose/raffinose mass ratios on the stability of co-lyophilized protein during storage above the T_g. Pharm Res 18:474–479.
111. Chang BS, Beauvais RM, Dong A, Carpenter JF. 1996. Physical factor affecting the storage stability of freeze-dried interleukin-1 receptor antagonist: Glass transition and protein conformation. Arch Biochem Biophys 331:249–258.
112. Franks F. 1990. Freeze drying: From empiricism to predictability. Cryo Lett 11:93–110.
113. Arakawa T, Kita Y, Carpenter JF. 1991. Protein-solvent interactions in pharmaceutical formulations. Pharm Res 8:285–291.
114. Kreilgaard L, Frokjaer S, Flink JM, Randolph TW, Carpenter JF. 1998. Effects of additives on the stability of recombinant human factor XIII during freeze-drying and storage in the dried solid. Arch Biochem Biophys 360:121–134.
115. Kreilgaard L, Frokjaer S, Flink JM, Randolph TW, Carpenter JF. 1999. Effects of additives on the stability of *Humicola Ianuginosa* lipase during freeze-drying and storage in the dried solids. J Pharm Sci 88:281–290.
116. Li S, Patapoff TW, Overcashier D, Hsu C, Nguyen T, Borchardt RT. 1996. Effects of reducing sugars on the chemical stability of human relaxin in the lyophilized state. J Pharm Sci 85:873–877.
117. Townsend MW, DeLuca PP. 1988. Use of lyoprotectants in the freeze-drying of a model protein, ribonuclease A. J Parenter Sci Technol 42:190–199.
118. Hageman MJ. 1988. The role of moisture in protein stability. Drug Dev Ind Pharm 14:2047–2070.
119. Lai MC, Topp EM. 1999. Solid-state chemical stability of proteins and peptides. J Pharm Sci 88:489–500.
120. Bell LN, Labuza TP. 1991. Aspartame degradation as a function of "water activity". Adv Exp Med Biol 302:337–349.
121. Bell LN, Hageman MJ. 1994. Differentiating between the effects of water activity and glass transition dependent mobility on a solid state chemical reaction: Aspartame degradation. J Agric Food Sci 42:2398–2401.
122. Yoshioka S, Aso Y, Otsuka T, Kojima S. 1995. Water mobility in poly(ethylene glycol)-,

DOI 10.1002/jps

poly(vinylpyrrolidone)-, and gelatin-water systems, as indicated by dielectric relaxation time, spin-lattice relaxation time, and water activity. J Pharm Sci 84:1072–1077.
123. Otsuka T, Yoshioka S, Aso Y, Kojima S. 1995. Water mobility in aquous solutions of macromolecular pharmaceutical excipients measured by oxygen-17 nuclear magnetic resonance. Chem Pharm Bull 43:1221–1223.
124. Aso Y, Yoshioka S, Terao T. 1994. Effect of binding of water to excipients as measured by ^{2}H-NMR relaxation time on cephalothin decomposition rate. Chem Pharm Bull 42:398–401.
125. Xiang T-X, Anderson BD. 2005. Distribution and effect of water content on molecular mobility in poly(vinylpyrrolidone) glasses: A molecular dynamics simulation. Pharm Res 22:1205–1214.
126. Aldous BJ, Franks F, Greer AL. 1997. Diffusion of water within an amorphous carbohydrate. J Mater Sci 32:301–308.
127. Tromp RH, Parker R, Ring SG. 1997. Water diffusion in glasses of carbohydrates. Carbohydr Res 303:199–205.
128. Oksanen CA, Zografi G. 1993. Molecular mobility in mixtures of absorbed water and solid poly-(vinylpyrrolidone). Pharm Res 10:791–799.
129. Shalaev EY, Shalaeva M, Byrn SR, Zografi G. 1997. Effects of processing on the solid-state methyl transfer of tetraglycine methyl ester. Int J Pharm 152:75–88.
130. Shalaev EY, Shalaeva M, Zografi G. 2002. The effect of disorder on the chemical reactivity of an organic solid, tetraglycine methyl ester: Change of the reaction mechanism. J Pharm Sci 91:584–593.
131. Tong P, Zografi G. 2003. Effects of water vapor absorption on the physical and chemical stability of amorphous sodium indomethacin. Pharm Sci Tech 5: Article 26.
132. Shalaev EY, Byrn SR, Zografi G. 1997. Single-phase and heterophase solid-state chemical kinetics of thermally induced methyl transfer in tetraglycine methyl ester. Int J Chem Kinet 29: 339–348.
133. Skwierczynski RD. 1999. Disorder, molecular mobility, and solid-state kinetics: The two-environment model. J Pharm Sci 88:1234–1236.
134. Fransson J, Florin-Robertsson E, Axelsson K, Nyhlén C. 1996. Oxidation of human insulin-like growth factor I in formulation studies: Kinetics of methionine oxidation in aqueous solution and in solid state. Pharm Res 13:1252–1257.

Available online at www.sciencedirect.com
ScienceDirect
International Journal of Pharmaceutics 336 (2007) 191–195
INTERNATIONAL JOURNAL OF PHARMACEUTICS
www.elsevier.com/locate/ijpharm

Note

Crystallization rate of amorphous nifedipine analogues unrelated to the glass transition temperature

Tamaki Miyazaki*, Sumie Yoshioka, Yukio Aso, Toru Kawanishi

National Institute of Health Sciences, 1-18-1 Kamiyoga, Setagaya-ku, Tokyo 158-0851, Japan

Received 14 August 2006; received in revised form 12 October 2006; accepted 18 November 2006
Available online 28 November 2006

Abstract

To examine the relative contributions of molecular mobility and thermodynamic factor, the relationship between glass transition temperature (T_g) and the crystallization rate was examined using amorphous dihydropyridines (nifedipine (NFD), *m*-nifedipine (*m*-NFD), nitrendipine (NTR) and nilvadipine (NLV)) with differing T_g values. The time required for 10% crystallization, t_{90}, was calculated from the time course of decreases in the heat capacity change at T_g. The t_{90} of NLV and NTR decreased with decreases in T_g associated with water sorption. The t_{90} versus T_g/T plots almost overlapped for samples of differing water contents, indicating that the crystallization rate is determined by molecular mobility as indicated by T_g. In contrast, differences in the crystallization rate between these four drugs cannot be explained only by molecular mobility, since the t_{90} values at a given T_g/T were in the order: NLV > NTR > NFD ≈ *m*-NFD. A lower rate was obtained for amorphous drugs with lower structural symmetry and more bulky functional groups, suggesting that these factors are also important. Furthermore, the crystallization rate of NTR in solid dispersions with poly(vinylpyrrolidone) (PVP) and hydroxypropyl methylcellulose (HPMC) decreased to a greater extent than expected from the increased T_g. This also suggests that factors other than molecular mobility affect the crystallization rate.

Keywords: Crystallization; Amorphous state; Nifedipine; Glass transition; Molecular mobility; Excipients

Preparation of poorly water-soluble pharmaceuticals into amorphous forms improves their solubility. However, amorphous solids are physically unstable because of their high energy state, and crystallization during storage presents a problem. The process of crystallization is known to comprise two major steps: nucleation and crystal growth, and the rates are generally governed by molecular mobility affecting the diffusion rate of molecules and thermodynamic factors such as the Gibbs free energy and nucleus/amorphous interfacial energy (Saleki-Gerhardt and Zografi, 1994; Hancock and Zografi, 1997; Rodríguez-Hornedo and Murphy, 1999; Andronis and Zografi, 2000; Ngai et al., 2000). Our previous studies demonstrated that the overall crystallization rate of nifedipine (NFD) for both the amorphous pure drug and solid dispersions with poly(vinylpyrrolidone) (PVP) had similar temperature dependence as the mean relaxation time calculated using the Adam-Gibbs-Vogel equation, suggesting that the molecular mobility of amorphous pharmaceuticals was one of the important factors affecting the crystallization rate (Aso et al., 2001, 2004). However, the crystallization rate of amorphous pharmaceuticals cannot be determined only by molecular mobility, as it has been reported that the susceptibility to crystallization of pharmaceuticals possessing quite different thermodynamic properties does not follow the order of the decrease in the glass transition temperature (T_g) (Zhou et al., 2002).

The purpose of the present study is to discuss the relative contributions of the molecular mobility and thermodynamic factors to the crystallization rates of dihydropyridines with different substituents, including NFD, *m*-nifedipine (*m*-NFD), nitrendipine (NTR) and nilvadipine (NLV) (Fig. 1). The overall crystallization rates of these drugs in the pure amorphous solids were measured under various relative humidity (RH) conditions to elucidate the effects of the substituents and water content on the crystallization rate. The crystallization rate of NTR was also determined in solid dispersions containing polymers (PVP and hydroxypropyl methylcellulose (HPMC)). Although some

* Corresponding author. Tel.: +81 3 3700 1141; fax: +81 3 3707 6950.
E-mail addresses: miyazaki@nihs.go.jp (T. Miyazaki), yoshioka@nihs.go.jp (S. Yoshioka), aso@nihs.go.jp (Y. Aso), kawanish@nihs.go.jp (T. Kawanishi).

0378-5173/$ – see front matter © 2006 Elsevier B.V. All rights reserved.
doi:10.1016/j.ijpharm.2006.11.052

	abbreviation	R_1	R_2	R_3	R_4
nifedipine	[NFD]	CH_3	CH_3	NO_2	H
m-nifedipine	[m-NFD]	CH_3	CH_3	H	NO_2
nitrendipine	[NTR]	CH_3	C_2H_5	H	NO_2
nilvadipine	[NLV]	CN	$(CH_3)_2CH$	H	NO_2

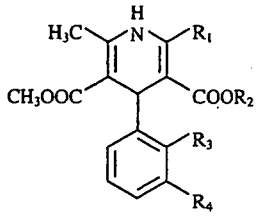

Fig. 1. Chemical structures of dihydropyridines.

papers have dealt with the crystallization of NTR and NLV in solid dispersions (Hirasawa et al., 2003a,b, 2004; Wang et al., 2005, 2006), few data are available that allow quantitative discussion about the relationship between molecular mobility and crystallization rates.

NFD and HPMC (USP grade) were purchased from Sigma Chemical Co. NTR, *m*-NFD and PVP (weight average molecular weight of 40000) were obtained from Wako Pure Chemical Industries Ltd. NLV was kindly supplied by Astellas Pharma Inc. The amorphous NFD, *m*-NFD, NTR, NLV and NTR solid dispersions with PVP and HPMC were prepared by melt quenching in the cell of a differential scanning calorimeter (DSC2920, TA Instruments). The crystalline drug or mixture of NTR and polymer (5 mg) was melted at a temperature approximately 20 °C above its melting point and then cooled to approximately 100 °C below the T_g at a cooling rate of 40 °C/min. Thermal and photo degradation of the drugs was checked by HPLC, and no change in the chromatograms was observed after the preparation in comparison with that before. Fig. 2 shows typical DSC thermograms for the four amorphous drugs immediately after preparation and after subsequent storage. The T_g values for the amorphous drugs were: NLV, 48.6 ± 0.3 °C; NFD, 46.2 ± 0.2 °C; *m*-NFD, 41.3 ± 0.1 °C; NTR, 32.4 ± 0.3 °C. As shown in Fig. 2(b), freshly prepared amorphous NFD exhibited two endothermic peaks at around 161 °C and 168 °C. The two melting points of the peaks agreed well with that for the metastable form II and stable form I, respectively (Burger and Koller, 1996). As shown in Fig. 2(c), the NFD sample, retaining an amorphous portion after 5 h storage at 60 °C, showed exothermic peaks due to crystallization of the amorphous phase and its transformation into a stable crystal, and melted at 168 °C, which is approximately the same temperature as the melting point of the intact crystal. As shown in Fig. 2(d), the sample stored at 60 °C for 46 h showed the exothermic peak around 120–140 °C due to transformation into a stable crystal, although change in the heat capacity (ΔC_p) at T_g was not significant. The exothermic peak around 120–140 °C due to transformation into a stable crystal was also observed during storage at 50 °C and 70 °C (thermogram not shown). These DSC thermograms suggested that amorphous NFD initially crystallized into a metastable form. Crystallization into the metastable form was also observed during storage at 50 °C and 70 °C (thermogram not shown). Amorphous *m*-NFD showed an exothermic peak due to crystallization but no obvious peak due to transformation into a stable form like that shown by the NFD samples, and melted at 206 °C, which is approximately the same temperature as the melting point of intact *m*-NFD (Fig. 2(f) and (g)). It is not clear from the DSC thermograms whether transition to a stable or a metastable crystalline form occurred during storage. Fig. 2(j) and (k) show the DSC thermograms of the partially crystallized NTR samples showing one melting peak at 128 °C. The observed melting point was lower than that of the stable crystal

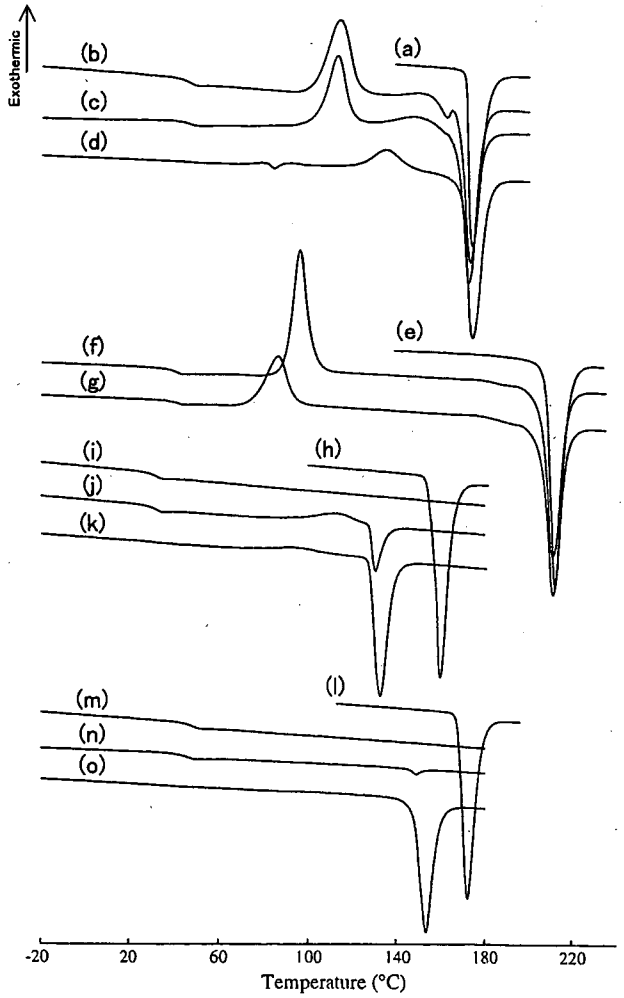

Fig. 2. Typical DSC thermograms: (a) NFD crystalline in the stable form, (b) freshly prepared amorphous NFD, (c) amorphous NFD after 5h-storage at 60 °C (d) amorphous NFD after 46 h-storage at 60 °C, (e) m-NFD crystalline in the stable form, (f) freshly prepared amorphous m-NFD, (g) amorphous m-NFD after 15 h-storage at 50 °C, (h) NTR crystalline in the stable form, (i) freshly prepared amorphous NTR, (j) amorphous NTR after 2 h-storage at 60 °C, (k) amorphous NTR after 9.75 h-storage at 60 °C, (l) NLV crystalline in the stable form, (m) freshly prepared amorphous NLV, (n) amorphous NLV after 48 h-storage at 80 °C, (o) amorphous NLV after 168 h-storage at 80 °C. Heating rate: 20 °C/min.

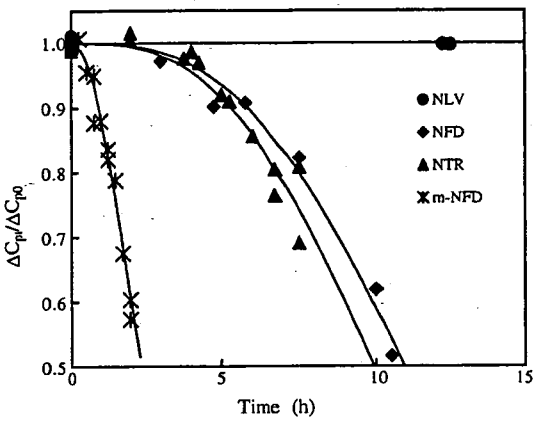

Fig. 3. Time profiles of crystallization for four dihydropyridines at 60 °C and 0%RH. The ratio of the amorphous form remaining at time t was calculated from the ΔC_p value assuming that the amount of amorphous phase is proportional to the ΔC_p. ΔC_{p0} and ΔC_{pt} are changes in ΔC_p at time 0 and t, respectively. Solid lines denote the fitting to the Avrami equation ($x(t) = \exp[-kt^n]$, $n = 3$).

(158 °C) and consistent with that reported for a metastable crystal (Kuhnert-Brandstätter and Völlenklee, 1986; Burger et al., 1997). As shown in Fig. 2(n) and (o), the partially crystallized NLV samples showed one melting peak at 148 °C. The observed melting point was lower than that for a stable crystal (168 °C) and similar to that for the dehydrated form of the monohydrate (Hirayama et al., 2000). Both amorphous NTR and NLV samples were considered to crystallize to their metastable crystalline forms under the conditions studied.

Fig. 3 shows the time profiles of crystallization of NFD, *m*-NFD, NTR, NLV at 60 °C and 0%RH. The crystallization rate was in the order: NLV < NTR = NFD < *m*-NFD. Fig. 4 shows the temperature dependence of the time required for 10% crystallization (t_{90}). Although NFD and NLV have approximately the same T_g, their values of t_{90} at the same temperature differed by more than two orders of magnitude (Fig. 4(A)). As shown in Fig. 4(B), the value of t_{90} at a given T_g/T (T being storage temperature) was in the order: NLV > NTR > NFD ≈ *m*-NFD within the whole range of temperature studied. As shown in Fig. 1, the four dihydropyridines have various alkyl groups at one of the carbonylester positions (R_2), and differ in the substitution position of the nitro group in the phenyl moiety (R_3 or R_4). The

Table 1
T_g values of amorphous NLV and NTR

RH (%)	T_g (°C)	
	NLV	NTR
0 (P_2O_5)	48.6 ± 0.3	32.4 ± 0.3
12 ($LiCl{\cdot}2H_2O$)	48.1 ± 0.7	30.5 ± 0.4
25 (CH_3COOK)	46.4 ± 0.5	29.0 ± 0.3
43 ($K_2CO_3{\cdot}2H_2O$)	43.4 ± 0.4	25.8 ± 0.3

For water absorption, the samples were kept at 5 °C for approximately 50 h in a desiccator containing saturated salt solutions. No crystallization was observed during the water absorption, as indicated by no endothermic melting peak in DSC thermograms.

bulkiness of R_2 shows the order: NFD, *m*-NFD (methyl) < NTR (ethyl) < NLV (isopropyl). Furthermore, the substituent at R_1 is a cyano group in NLV, whereas it is a methyl group in the other three drugs; thus, the structural symmetry of NLV is lower. Since the plots for NFD and *m*-NFD in Fig. 4(B) almost overlapped each other, the difference in the crystallization rate may be attributed to the difference in molecular mobility. In contrast, differences in the crystallization rate between NLV, NTR and NFD cannot be explained only by the difference in molecular mobility. The differences in structural symmetry and bulkiness of functional group may cause differences in the Gibbs free energy and nucleus/amorphous interfacial energy, resulting in the differing crystallization rates between these drugs.

The crystallization rate of amorphous NLV and NTR solids with differing T_g values due to differing water content was measured to elucidate the effect of T_g on the crystallization rate (Table 1). The partially crystallized NLV and NTR in the presence of water showed an endothermic melting peak at approximately 150 °C and 130 °C, respectively. This suggests that amorphous NLV and NTR containing water also crystallize into their metastable forms in a similar manner as shown for dry samples. Fig. 5(A) shows the temperature dependence of the t_{90} obtained for NLV and NTR in the presence of water. When compared at the same temperature, the t_{90} value decreased with increasing RH. As shown in Fig. 5(B), the t_{90} versus T_g/T plots for each drug overlapped with those obtained under dry conditions, suggesting that the effect of water on the t_{90} value was explainable by the plasticizing effect of absorbed water,

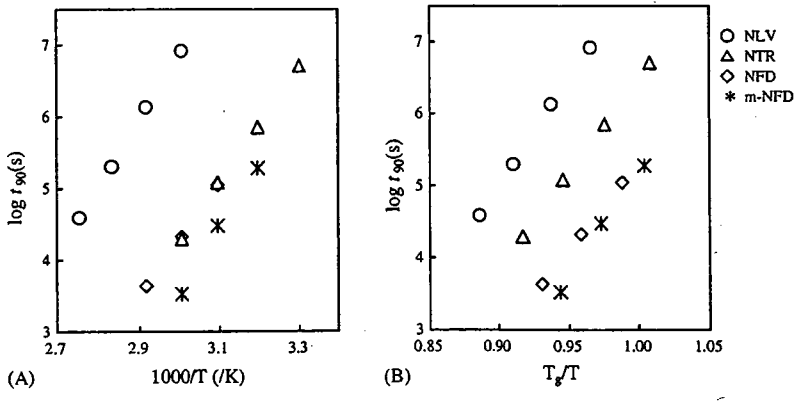

Fig. 4. Relationship between t_{90} for crystallization of drugs and storage temperature under dry conditions.

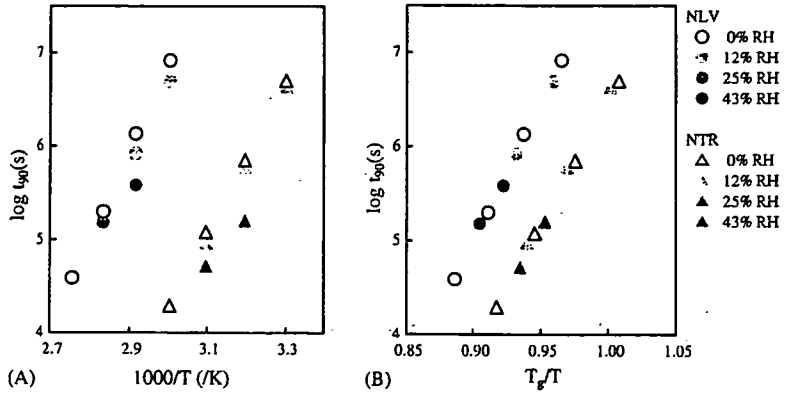

Fig. 5. Effect of absorbed water on the t_{90} of crystallization for NLV (circles) and NTR (triangles). The t_{90} values were measured at the early stage of crystallization at which no marked change in Tg was evident.

Table 2
T_g values of NTR-polymer solid dispersions

Polymer (%)	T_g (°C)	
	PVP	HPMC
0	32.4 ± 0.3	
3	33.2 ± 0.2	32.4 ± 0.1
5	34.1 ± 0.3	32.9 ± 0.4
6	34.1 ± 0.3	32.8 ± 0.2
11	36.6 ± 0.3	33.4 ± 0.3
20	–	33.7 ± 0.7
23	43.4 ± 0.8	–

similarly to that reported for NFD crystallization (Aso et al., 1995).

The effect of T_g on the crystallization rate of NTR was also investigated in solid dispersions with PVP and HPMC. A single T_g was observed for amorphous NTR-polymer solid dispersions prepared with 2.7–23% polymer excipients, indicating that NTR and polymer are miscible within the sensitivity limit of the DSC method. The value of T_g tended to increase with the amount of polymer, and the extent of increase was greater for NTR-PVP dispersions than for NTR-HPMC dispersions (Table 2). As the partially crystallized NTR-polymer dispersions showed a melt-

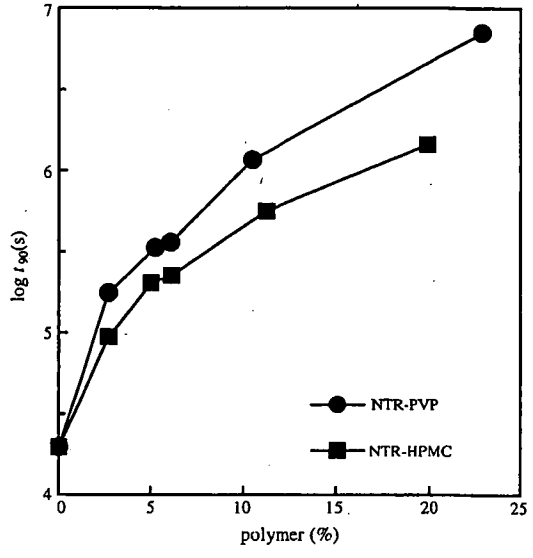

Fig. 6. Effect of polymer content on crystallization of NTR in solid dispersions with PVP and HPMC at 60 °C and 0%RH.

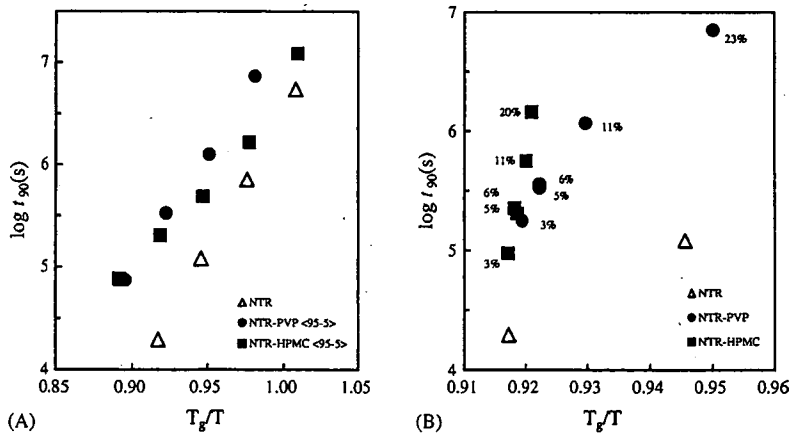

Fig. 7. Relationship between T_g/T and t_{90} of crystallization for NTR in the pure amorphous form and solid dispersions with PVP and HPMC. Numbers in percentage terms in figure (B) denote polymer contents.

ing peak at approximately 130 °C, the crystallization of NTR in the presence of the polymers was considered to be transition into a metastable form in a similar manner as that observed for pure amorphous NTR. Fig. 6 shows the effect of polymer excipients on the t_{90} values. Both PVP and HPMC increased t_{90} as the amount of polymer increased, but PVP was more effective in stabilizing amorphous NTR within the range of content studied. Fig. 7(A) shows the temperature dependence of t_{90} for solid dispersions containing 5% polymer. The t_{90} value compared at the same T_g/T was longer for both NTR-polymer dispersions than for pure NTR. Furthermore, the t_{90} versus T_g/T plots for solid dispersions containing various amounts of polymers did not overlap with that for pure NTR (Fig. 7(B)), indicating that crystallization of NTR was inhibited by the addition of PVP and HPMC to a greater extent than expected from the increased T_g. The present results imply that the drug-polymer interaction as well as an antiplasticizing effect of polymer excipients retarded the crystallization of the amorphous solid (Hirasawa et al., 2003a,b, 2004; Aso et al., 2004; Miyazaki et al., 2004, 2006; Wang et al., 2006).

Acknowledgement

A part of this work was supported by a grant from the Japan Health Science Foundation.

References

Andronis, V., Zografi, G., 2000. Crystal nucleation and growth of indomethacin polymorphs from the amorphous state. J. Non-Cryst. Solids 271, 236–248.

Aso, Y., Yoshioka, S., Otsuka, T., Kojima, S., 1995. The physical stability of amorphous nifedipine determined by isothermal microcalorimetry. Chem. Pharm. Bull. 43, 300–303.

Aso, Y., Yoshioka, S., Kojima, S., 2001. Explanation of the crystallization rate of amorphous nifedipine and Phenobarbital from their molecular mobility as measured by ^{13}C nuclear magnetic resonance relaxation time and the relaxation time obtained from the heating rate dependence of the glass transition temperature. J. Pharm. Sci. 90, 798–806.

Aso, Y., Yoshioka, S., Kojima, S., 2004. Molecular mobility-based estimation of the crystallization rates of amorphous nifedipine and Phenobarbital in poly(vinylpyrrolidone) solid dispersions. J. Pharm. Sci. 93, 384–391.

Burger, A., Koller, K.T., 1996. Polymorphism and pseudopolymorphism on nifedipine. Sci. Pharm. 64, 293–301.

Burger, A., Rollinger, J.M., Brüggeller, P., 1997. Binary system of (*R*)- and (*S*)-nitrendipine—polymorphism and structure. J. Pharm. Sci. 86, 674–679.

Hancock, B.C., Zografi, G., 1997. Characteristics and significance of the amorphous state in pharmaceutical systems. J. Pharm. Sci. 86, 1–12.

Hirasawa, N., Ishise, S., Miyata, H., Danjo, K., 2003a. Physicochemical characterization and drug release studies of Nilvadipine solid dispersions using water-insoluble polymer as a carrier. Drug Dev. Ind. Pharm. 29, 339–344.

Hirasawa, N., Ishise, S., Miyata, H., Danjo, K., 2003b. An attempt to stabilize Nilvadipine solid dispersion by the use of ternary systems. Drug Dev. Ind. Pharm. 29, 997–1004.

Hirasawa, N., Ishise, S., Miyata, H., Danjo, K., 2004. Application of Nilvadipine solid dispersion to tablet formulation and manufacturing using crospovidone and methylcellulose as dispersion carriers. Chem. Pharm. Bull. 52, 244–247.

Hirayama, F., Honjo, M., Arima, H., Okimoto, K., Uekama, K., 2000. X-ray crystallographic characterization of Nilvadipine monohydrate and its phase transition behavior. Eur. J. Pharm. Sci. 11, 81–88.

Kuhnert-Brandstätter, M., Völlenklee, R., 1986. Beitrag zur polymorphie von arzneistoffen 2. Mitteilung: halofenat, lorcainidhydrochlorid, minoxidil, mopidamol und nitrendipin. Sci. Pharm. 54, 71–82.

Miyazaki, T., Yoshioka, S., Aso, Y., Kojima, S., 2004. Ability of polyvinylpyrrolidone and polyacrylic acid to inhibit the crystallization of amorphous acetaminophen. J. Pharm. Sci. 93, 2710–2717.

Miyazaki, T., Yoshioka, S., Aso, Y., 2006. Physical stability of amorphous acetanilide derivatives improved by polymer excipients. Chem. Pharm. Bull. 54, 1207–1210.

Ngai, K.L., Magill, J.H., Plazek, D.J., 2000. Flow, diffusion and crystallization of supercooled liquids: revisited. J. Chem. Phys. 112, 1887–1892.

Rodríguez-Hornedo, N., Murphy, D., 1999. Significance of controlling crystallization mechanisms and kinetics in pharmaceutical systems. J. Pharm. Sci. 88, 651–660.

Saleki-Gerhardt, A., Zografi, G., 1994. Non-isothermal and isothermal crystallization of sucrose from the amorphous state. Pharm. Res. 11, 1166–1173.

Wang, L., Cui, F.D., Hayase, T., Sunada, H., 2005. Preparation and evaluation of solid dispersion for Nitrendipine-carbopol and Nitrendipine-HPMCP systems using a twin screw extruder. Chem. Pharm. Bull. 53, 1240–1245.

Wang, L., Cui, F.D., Sunada, H., 2006. Preparation and evaluation of solid dispersions of Nitrendipine prepared with fine silica particles using the melt-mixing method. Chem. Pharm. Bull. 54, 37–43.

Zhou, D., Zhang, G.G.Z., Law, D., Grant, K.J.W., Schmitt, E.A., 2002. Physical stability of amorphous pharmaceuticals: importance of configurational thermodynamic quantities and molecular mobility. J. Pharm. Sci. 91, 1863–1872.

Miscibility of Nifedipine and Hydrophilic Polymers as Measured by ^{1}H-NMR Spin–Lattice Relaxation

Yukio Aso,*[a] Sumie Yoshioka,[a] Tamaki Miyazaki,[a] Tohru Kawanishi,[a] Kazuyuki Tanaka,[b] Satoshi Kitamura,[b] Asako Takakura,[c] Takashi Hayashi,[c] and Noriyuki Muranushi[c]

[a] *National Institute of Health Sciences; 1–18–1 Kamiyoga, Setagaya-ku, Tokyo 158–8501, Japan:* [b] *Astellas Pharma Inc.; 180 Ozumi, Yaizu, Shizuoka 425–0072, Japan: and* [c] *Shionogi & Co., Ltd.; 2–1–3 Kuise, Terajima, Amagasaki, Hyogo 660–0813, Japan.* Received April 19, 2007; accepted June 4, 2007; published online June 5, 2007

The miscibility of a drug with excipients in solid dispersions is considered to be one of the most important factors for preparation of stable amorphous solid dispersions. The purpose of the present study was to elucidate the feasibility of ^{1}H-NMR spin–lattice relaxation measurements to assess the miscibility of a drug with excipients. Solid dispersions of nifedipine with the hydrophilic polymers poly(vinylpyrrolidone) (PVP), hydroxypropylmethylcellulose (HPMC) and α,β-poly(*N*-5-hydroxypentyl)-L-aspartamide (PHPA) with various weight ratios were prepared by spray drying, and the spin–lattice relaxation decay of the solid dispersions in a laboratory frame (T_1 decay) and in a rotating frame ($T_{1\rho}$ decay) were measured. $T_{1\rho}$ decay of nifedipine–PVP solid dispersions (3 : 7, 5 : 5 and 7 : 3) was describable with a mono-exponential equation, whereas $T_{1\rho}$ decay of nifedipine–PHPA solid dispersions (3 : 7, 4 : 6 and 5 : 5) was describable with a bi-exponential equation. Because a mono-exponential $T_{1\rho}$ decay indicates that the domain sizes of nifedipine and polymer in solid dispersion are less than several nm, it is speculated that nifedipine is miscible with PVP but not miscible with PHPA. All the nifedipine–PVP solid dispersions studied showed a single glass transition temperature (T_g), whereas two glass transitions were observed for the nifedipine–PHPA solid dispersion (3 : 7), thus supporting the above speculation. For nifedipine–HPMC solid dispersions (3 : 7 and 5 : 5), the miscibility of nifedipine and HPMC could not be determined by DSC measurements due to the lack of obviously evident T_g. In contrast, ^{1}H-NMR spin–lattice relaxation measurements showed that nifedipine and HPMC are miscible, since $T_{1\rho}$ decay of the solid dispersions (3 : 7, 5 : 5 and 7 : 3) was describable with a mono-exponential equation. These results indicate that ^{1}H-NMR spin–lattice relaxation measurements are useful for assessing the miscibility of a drug and an excipient in solid dispersions.

Key words miscibility; solid dispersion; spin diffusion; spin–lattice relaxation time; amorphous

Preparing solid dispersions of a poorly soluble drug with water-soluble polymers is a promising method for improving the dissolution characteristics and bioavailability of the drug. Miscibility between a drug and a polymer is considered to be one of the most important factors for obtaining stable solid dispersions.[1)]

Miscibility of a drug with a polymer is usually evaluated by differential scanning calorimetry (DSC).[2—6)] When a solid dispersion shows a single glass transition temperature (T_g) between the T_g values of the drug and the polymer, the drug and the polymer are considered to be miscible within the detection limit of DSC.[7)] This method is applicable to a solid dispersion when T_g of the drug and the polymer can be detected clearly, and the temperature ranges of the base line shift due to glass transition do not overlap each other.

The interaction parameter χ of the Flory–Huggins equation provides a measure of miscibility.[8,9)] Crowly and Zografi measured the water vapor sorption isotherm of indomethacin solid dispersions with PVP and reported that the estimated interaction parameter χ between indomethacin and PVP was greater than 0.5, indicating that indomethacin and PVP are immiscible in terms of χ value.[8)] Although this method is excellent in being able to provide a quantitative measure of miscibility, it may be difficult to apply to unstable amorphous drugs, which crystallize during measurement of water vapor sorption.

A method that can be used as an alternative to DSC or measurement of the interaction parameter χ is analysis of the ^{1}H spin–lattice relaxation process of solid dispersions, which has been reported in the fields of polymer alloy and polymer blends. If two polymers are miscible, the relaxation decay of the mixture is describable by a mono-exponential equation, whereas if they are not miscible, relaxation decay is describable by a bi-exponential equation.[10,11)]

In this paper, the feasibility of ^{1}H spin–lattice relaxation measurements for evaluating the miscibility of a drug and polymers in solid dispersions was studied. Nifedipine solid dispersions with PVP, HPMC and α,β-poly(*N*-5-hydroxypentyl)-L-aspartamide (PHPA) were used as model solid dispersions, and the miscibility measured by ^{1}H-NMR was compared with that measured by DSC. The dissolution profiles of nifedipine from PVP solid dispersions were compared with those from PHPA solid dispersions to discuss the effects of miscibility on the dissolution rate of nifedipine.

Theory ^{1}H spin–lattice relaxation rates of respective spins in a solid are usually averaged by a process called spin diffusion. Spin diffusion is the equilibration process of polarizations of spins at different local sites through mutual exchange of magnetization. ^{1}H spin–lattice relaxation decay for a single-phase solid is describable by a mono-exponential equation with a relaxation rate that is averaged by spin diffusion. When a solid consists of two phases, the spin–lattice relaxation decay is describable by a mono-exponential or a bi-exponential equation depending on both the domain size of each phase and the effective diffusion length (L). L is expressed as follows:

$$L=\sqrt{6Dt} \quad (1)$$

* To whom correspondence should be addressed. e-mail: aso@nihs.go.jp

where D is the spin diffusion coefficient, and t is the diffusion time. D is a function of the distance between neighboring proton spins and spin–spin relaxation time (T_2), and is reported to be approximately 10^{-12} cm^2 s^{-1} for organic polymers. Typical spin–lattice relaxation time in a laboratory frame (T_1) and that in a rotating frame ($T_{1\rho}$) are of the order of 1 s and 10 ms, respectively. When these values for t were inserted in Eq. 1, effective diffusion lengths of approximately 50 nm and 5 nm were obtained for T_1 and $T_{1\rho}$, respectively. Depending on the domain size of each phase in a solid, the following 3 cases can be expected: (1) when the domain is smaller than about 5 nm, both the spin–lattice relaxation decay patterns in a laboratory frame (T_1 decay) and in a rotating frame ($T_{1\rho}$ decay) are describable by a mono-exponential equation; (2) when the domain size is about 5 to 50 nm, the $T_{1\rho}$ decay pattern is describable by a bi-exponential equation, whereas the T_1 decay pattern is describable by a mono-exponential equation; and (3) when the domain size is larger than about 50 nm, both the T_1 and $T_{1\rho}$ decay patterns are describable by a bi-exponential equation. When the $T_{1\rho}$ decay is describable by a mono-exponential equation, the solid can be considered as a single phase within the detection limit of NMR. T_1 and $T_{1\rho}$ decay thus provide information on miscibility of a drug and a polymer excipient.[11]

Experimental

Materials Nifedipine (N-7634), PVP (PVP-40) and HPMC (H-3785) were purchased from Sigma (Newcastle, DE, U.S.A.). PHPA was synthesized *via* polycondensation of L-aspartic acid.[12] Phenobarbital was obtained from sodium phenobarbital (Wako Pure Chemical Ind., Osaka) by neutralization and subsequent re-crystallization from acetone solutions as described previously.[13] Other chemicals used were of reagent grade. Nifedipine solid dispersions with PVP, HPMC and PHPA were prepared by a solvent evaporation method using a model GS-310 spray dryer (Yamato, Tokyo, Japan). Drying conditions are summarized in Table 1. The solid dispersions obtained were confirmed to be amorphous from microscopic observation under polarized light. Although the drying conditions were not optimized, 50 to 90% of the solid dispersions were obtained. Amorphous nifedipine was prepared by melting and subsequent rapid cooling as reported previously.[14]

DSC T_g of nifedipine–PVP and nifedipine–HPMC solid dispersions was measured by modulated temperature DSC using a model 2920 differential scanning calorimeter and a refrigerator cooling system (TA Instruments, Newcastle, DE, U.S.A.). The modulated temperature program used was a modulation amplitude of ±0.5 °C, a modulation period of 100 s and an underlying heating rate of 1 °C/min. For nifedipine–PHPA solid dispersions, T_g was measured at a scanning rate of 20 °C/min using a conventional heating program. Temperature calibration of the instrument was carried out using indium.

NMR T_1 decay and $T_{1\rho}$ decay were measured using a model JNM-MU25 pulsed NMR spectrometer (JEOL DATUM, Tokyo, Japan). The inversion recovery pulse sequence was used to measure T_1 decay. $T_{1\rho}$ decay was measured in a spin locking field of 10 G. All measurements were carried out at 27 °C.

X-Ray Powder Diffraction X-Ray powder diffraction patterns of solid dispersions were obtained using a model RINT-TTR II X-ray diffractometer (Rigaku Denki, Tokyo) with Cu$K\alpha$ radiation (50 kV, 300 mA) at a scanning rate of 4 °C/min from 2θ=5° to 40°.

Nifedipine Dissolution Profile Nifedipine–PVP (3 : 7) and nifedipine–PHPA (3 : 7) solid dispersions containing 100 mg of nifedipine were made into disks with a diameter of 2 cm at a pressure of 20 kN. Each disk was mounted on the rotor of the dissolution apparatus and the side surface of the disk was covered with a Teflon film. The sample was rotated at a rate of 100 rpm in 900 ml of distilled water at 37 °C. The amount of nifedipine dissolved was measured using a model DM-3100 solution monitor (Otsuka Electronics, Tokyo).

Results and Discussion

Figure 1 shows typical T_1 and $T_{1\rho}$ decay patterns for the solid dispersion and the physical mixture of nifedipine and PHPA (3 : 7). T_1 and $T_{1\rho}$ decay patterns were mono-exponential for both amorphous nifedipine and PHPA. The T_1 and $T_{1\rho}$ values of nifedipine were 5.0 s and 104 ms, respectively, and those of PHPA were 0.084 s and 4.4 ms, respectively. The physical mixture of nifedipine and PHPA (3 : 7) exhibited bi-exponential T_1 and $T_{1\rho}$ decay with the relaxation time of each component, indicating that the particle sizes of nifedipine and PHPA in the physical mixture are much larger than the effective diffusion length (approximately 5 nm and 50 nm for $T_{1\rho}$ and T_1 decay, respectively). In contrast to the physical

Table 1. Conditions of Spray Drying

Drug	Polymer	Solvent[a]	Outlet temperature (°C)	Atomizer gas (l/min)	Feeding rate (ml/min)
Nifedipine–PHPA					
0	10	A	68	7	5
3	7	A	68	7	3
4	6	A	68	7	3
5	5	A	68	7	3
Phenobarbital–PHPA					
3	7	A	68	7	3
Nifedipine–PVP					
0	10	A	90	9	10
3	7	A	90	9	10
5	5	A	90	9	10
7	3	A	68	7	3
Nifedipine–HPMC					
0	10	B	38	11	3
3	7	B	38	11	2
5	5	B	38	11	2
7	3	B	38	11	4

a) Solvent A, ethanol; solvent B, ethanol–CH_2Cl_2 (1 : 1). Flow rate of drying gas was adjusted to 0.5 m^3/min.

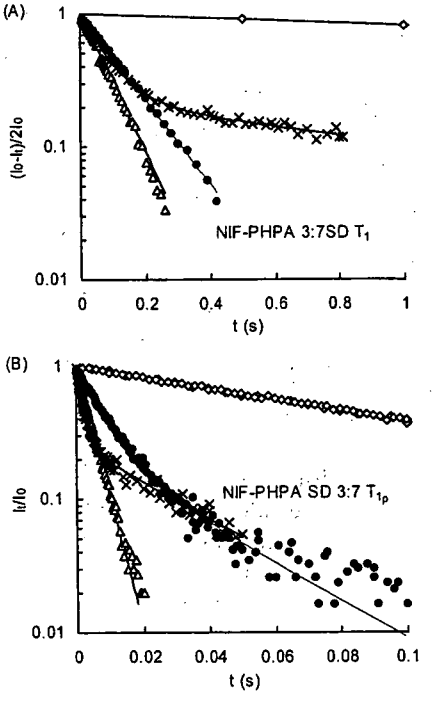

Fig. 1. T_1 (A) and $T_{1\rho}$ (B) Decay Patterns for Amorphous Nifedipine (◇), Amorphous PHPA (△), Physical Mixture (×) and Solid Dispersions (●) of Nifedipine and PHPA